



TiAlN Thin Films: Growth, Characterization and Hydrophobia the Surface of the Steel Using Low Energy Plasma Focus Device

Hasan Anousha^{1*}, Eslam Ghareshabani²

¹ MS.c in Physics - Atomic and Molecular, Department of Physics, Faculty of Basic Sciences, Sahand University of Technology, Tabriz, Iran

² Associate Professor of Physics, Sahand University of Technology, Tabriz, Iran.

***Corresponding Author**

Abstract: In this experimental study, a 1.5kJ Plasma Focus device of Mather type was employed to grow Titanium Aluminum Nitride (TiAlN) coatings at room temperature on 316 Stainless Steel sub-layer. The anode of the device was made of Ti and Al. A mixture of N₂ and Ar gases was used as the work gas for TiAlN deposition. TiAlN Nano-particles were formed on stainless steel with 0° of the degree with respect to the anode axis by different shots at 5cm above the anode. X-ray Diffraction (XRD) results indicated the formation of the TiAlN structure on stainless steel. Scanning Electron Microscopy (SEM) images demonstrated the approximately uniform growth of TiAlN Nano-particles on the surface. EDX analysis results showed that an increase in the number of the shots increased the deposition of TiAlN on the sub-layer. According to the Atomic Force Microscopy (AFM) images, the mean thickness of the surface increased as the shots increased in number. Contact Angle analysis shows the contact angle between the droplet and the steel substrate surface 44.54° and the contact angle between the droplet and the surface of deposited TiAlN nanoparticles 100.62°. Micro-hardness test results of the thin layers showed that an increase in the number of the shots increased the hardness of the samples.

Keywords: TiAlN, Plasma Focus, Thin Films, XRD, AFM, Contact Angle.

INTRODUCTION

Titanium Aluminum Nitride (TiAlN) is a refractory and very hard material. Due to its physical and chemical properties, from high temperature resistance to corrosion resistance, it is widely used for coating in high-temperature technologies (Liu et al., 2005). TiAlN consists of Titanium and Aluminum and has the following advantages over Titanium Nitride:

- 1) Oxidation resistance at high temperatures (800-900°C) due to the formation of the protective aluminum oxide layer;
- 2) Higher hardness (3000 HV);
- 3) Lower electrical and thermal conductivity (Liu et al., 2005; Aleksandar et al., 2018; Tousif et al., 2011).

TiAlN coatings have wurtzite structure at a high Al portion over Ti, while they are in form of NaCl-B1 at a high Ti portion over Al (Fig 1).

TiAlN Nano-particles have been deposited by different methods among which are Physical Vapor Deposition (PVD) (Vikas Chawla et al., 2011; Ahlgren and Blomqvist, 2005; Kim, Lee and Hahn, 2005), Sputtering (Shum et al., 2004; Lee et al., 2007), Chemical Vapor Deposition (CVD) (Wagner et al., 2008), and Laser/Sol Gel Method. TiAlN particles have also been formed by other plasma focus devices with different energy and configuration (Hosseinnejad et al., 2011; Rawat et al., 2001).

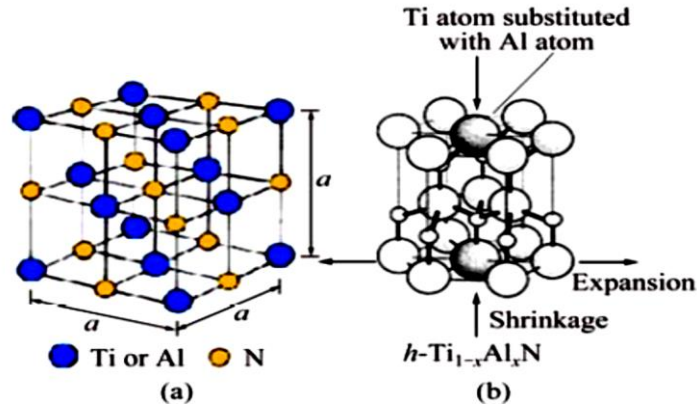


Figure 1: TiAlN Lattice Structure for a) B1-NaCl and b) Wurtzite

In this study, the plasma focus device of Tabriz Sahand University of Technology was employed to grow TiAlN Nano-particles on stainless steel sub-layer. The Nano-particles were formed on the stainless steel with different numbers of shots. The synthesized samples were examined in their structure by XRD, in surface morphology by SEM, in elements dispersion on the sub-layer by Mapping Analysis, in topography and surface thickness by AFM, and in grown elements combination on the sub-layer by EDX. Then, by roughness and low surface energy nanoparticle layer deposition, the intended surface becomes hydrophobic.

Methodology

Mather Plasma Focus device of Tabriz Sahand University of Technology consisted of a copper anode electrode with 1.8cm of diameter and 5.3cm of length, surrounded by 6 bronze cathode electrodes, each with 5.3cm of length. A Pyrex insulator has separated the electrodes (Fig 2). In this experiment, the anode was made of Ti and Al. There was a shutter between the anode electrode and the sample holder for the initial shots to achieve an excellent pinch. The entire set of the electrodes were inside a vacuum container that was pressure-dropped by a rotary compressor to 0.2torr. Then, a mix of N_2 and Ar gases was injected inside the vacuum container as the working gas.

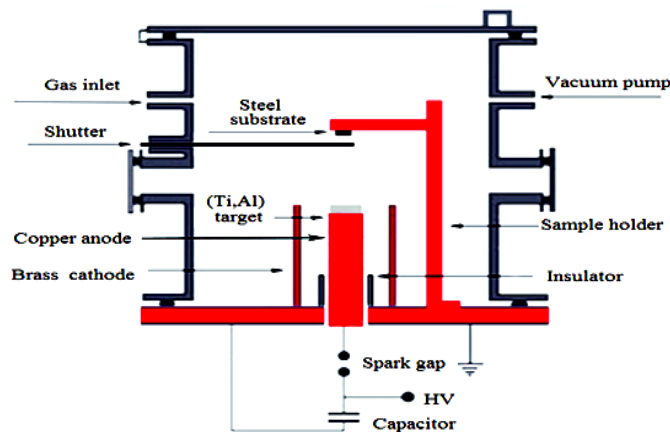


Figure 2. Schematic of Mather Plasma Focus Device

The optimum pressure for the excellent pinch in the experiment was 0.2torr at 6kV of voltage. The voltage wave form versus current at pinch time, which was received from Rogowsky coil, was recorded by an oscilloscope (Fig 3).

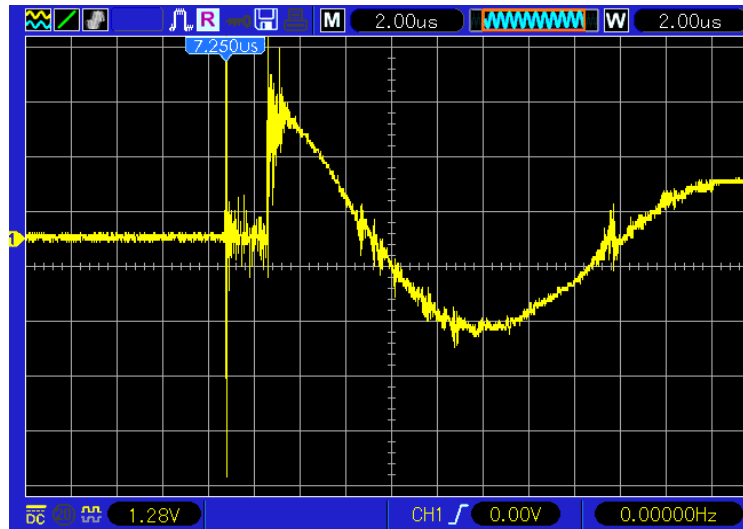


Figure 3: Rogowsky Coil Current Derivative Signal at Pinch Time

For the operation of the plasma focus device, a high voltage was applied between two anode and cathode electrodes by three 10 μ F capacitors charged by a high voltage. Then, an electrical discharge took place on the insulator surface in 100ns, creating a current layer on the insulator surface. A self-consistent magnetic field is created, producing Lorentz force and accelerating the current layer to the open end of the anode. As a result, the $J \times B$ force compressed the current layer on the anode, which created warm dense plasma. At this time, the plasma column created by the sausage instability ($m=0$) was eliminated by the production of high-energy electron, ion, and X-ray particles. Since a strong magnetic field was created when the plasma column was eliminated, this magnetic field accelerated the ions and electrons in opposite directions such that the high-energy electrons collided with the anode (Ti, Al) and resulted in their melt. Ti and Al atoms were mixed with the ionized N_2 gas and deposited on the sub-layer at the pinch time by the produced plasma jet (Fig 4). Before the formation of the Nano-particles, steel samples were cleaned with alcohol, acetone, and distilled water, each for 20 minutes in an ultrasonic device with the help of ultrasonic waves.

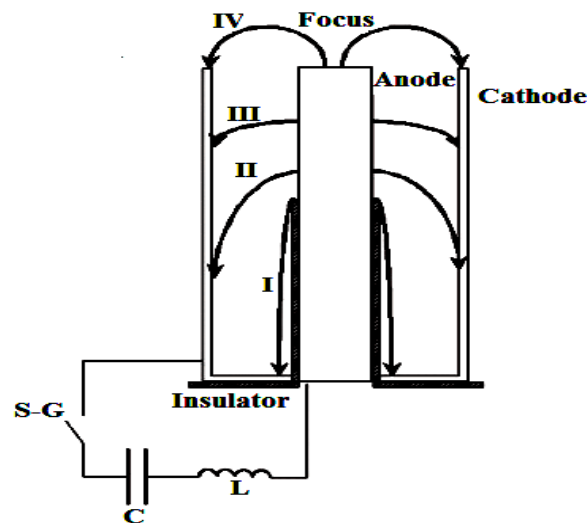


Fig. 4 Dynamics of the Plasma Focus Device

The samples were placed 5cm above the anode. (Ti,Al)N Nano-particles were also placed at 0° with respect to the anode axis with 100, 150, and 200 shots, being analyzed by XRD, SEM, AFM, EDX, and Mapping devices.

X-ray Spectroscopy Results

The XRD spectroscopy of the samples was done using Grazing technique which is specific to thin layers and coatings. Figure 5 represents the X-ray diffraction spectrum of the synthesized samples with different shots. The diffraction spectrum shows the formation of the TiAlN crystalline phase for the samples grown on steel. Different peaks of TiAlN crystalline planes were observed at 2θ of 44.3°, 51.9°, and 75.6° along with Al₂O₃ at 45.7°. The diffraction peak locations is matched with the standard data for TiAlN. Hence, the patterns indicate the growth of TiAlN crystals on steel.

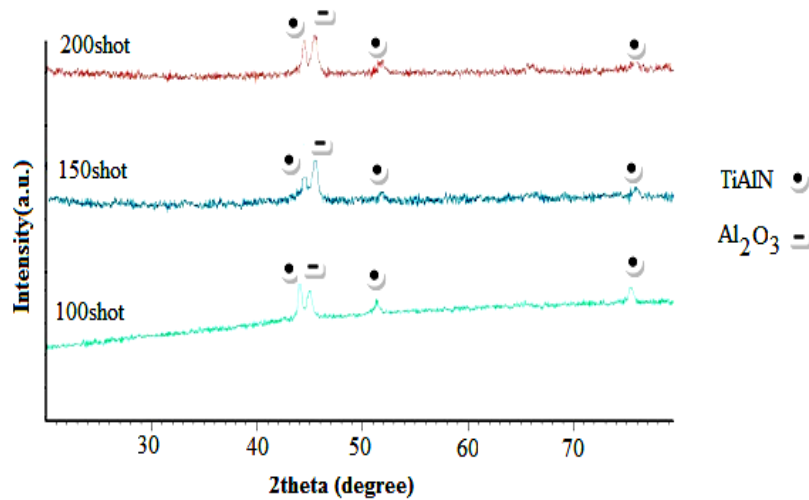


Figure 5: X-ray Diffraction Spectrum for the Samples Synthesized with a) 100 shots, b) 150 shots, and c) 200 shots

The average size of TiAlN was measured by Scherrer formula in equation 1, where λ is a wavelength of Cu Kα radiation 0.154 nm, D is the size of the crystal, β is FWHM, and K is Scherrer constant, in this case, was 0.9. From this formula, The average particle size of 100, 150 and 200 shots is 47, 52 and 100 nm, respectively

$$d = \frac{0.9\lambda}{\beta \cos\theta} \quad (1)$$

SEM Results

Figure 6 demonstrates the SEM images for TiAlN Nano-particles on the steel sub-layer. These particles are almost uniformly distributed on the surface. As it is observed, the increased number of the shots increased the deposition on the sub-layer, with the particles starting to join together. The size of the Nano-particles has been increased at 200 shots, which can be attributed to the increased surface energy due to the increased shot number and deposition.

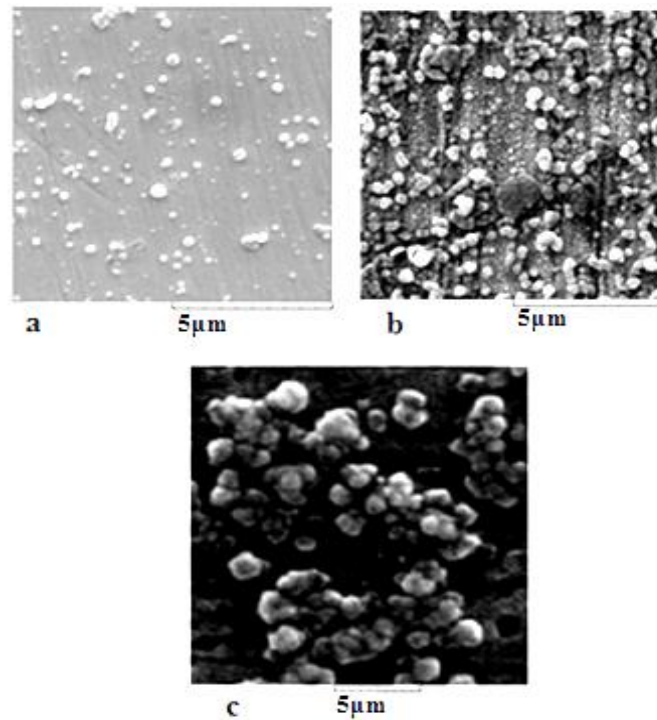


Figure 6: SEM Images at a) 100 shots, b) 150 shots, c) 200 shots

AFM Results

To measure roughness of the surface of the samples, a microscope of atomic force is used in non-contact state and with a sharp needle of about 2 μm and a diameter of less than 10 nm. The AFM images in 5×5 μm dimensions show that an increase in the number of the shots from 100 to 200, the Nano-particles size is increased from $40 \pm 10 \text{ nm}$ to $90 \pm 10 \text{ nm}$ which is corresponded with the XRD results. The mean surface thickness was 188 nm at 100 shots, which was increased to 359 nm as the number of the shots increased to 200. This can be due to the increased energy of the ions thrown toward the sub-layer (Fig 7).

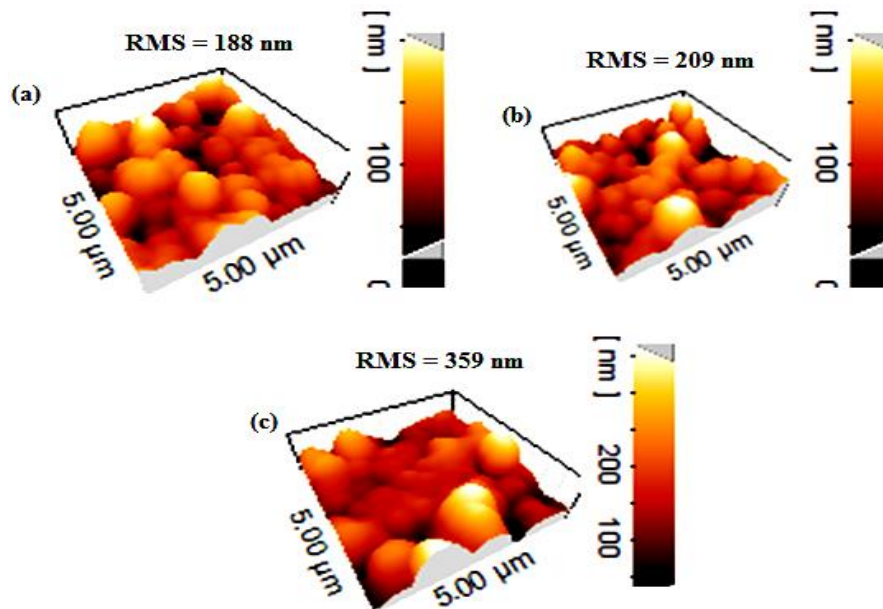


Figure 7 AFM Images for the Nano-particles Grown at a) 100 shots, b) 150 shots, and c) 200 shots

EDX Results

EDX analysis was employed to identify the elements constituting the samples. Figure 8 shows the EDX spectroscopy of the elements grown on the sub-layer at different number of shots. EDX results indicate that an increase in the number of the shots affects TiAlN grown on the sub-layer – i.e. it increases TiAlN deposition. At 100 shots, a high content of TiAlN atoms do not have sufficient energy to reach the sub-layer and grow on it due to their high weights and low velocities. Another reason is that the atoms separated from the anode surface are conically dispersed when the focus collapses and the number of TiAlN atoms getting vertically close to the sub-layer is decreased.

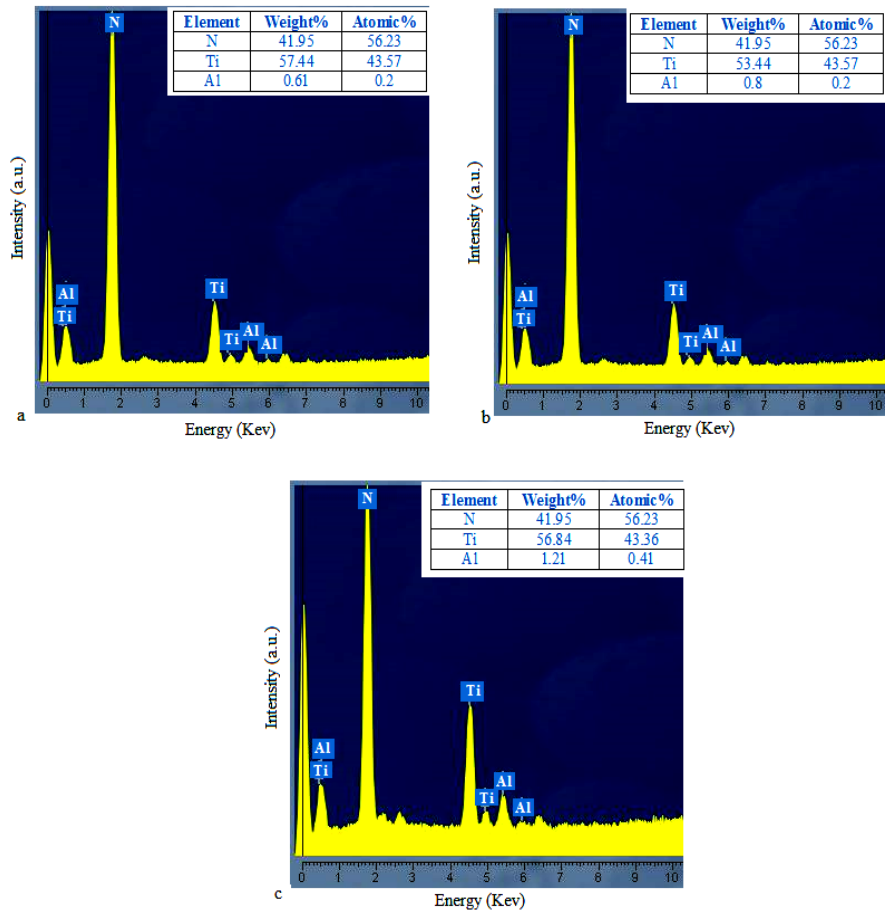


Figure 8: the EDX spectroscopy of the Elements Deposited on the Sub-layer at a) 100, b) 150, and c) 200 shots

Mapping Results

This analysis was done to measure the uniformity of the thin layer and investigate the dispersion of the elements on the sub-layer by SEM, in which the locations of the deposited atoms on the sub-layer are indicated by the device. Figure 9 represents Ti, Al, and N atoms on the steel sub-layer. Mapping results show TiAlN deposition as uniform on the sub-layer.

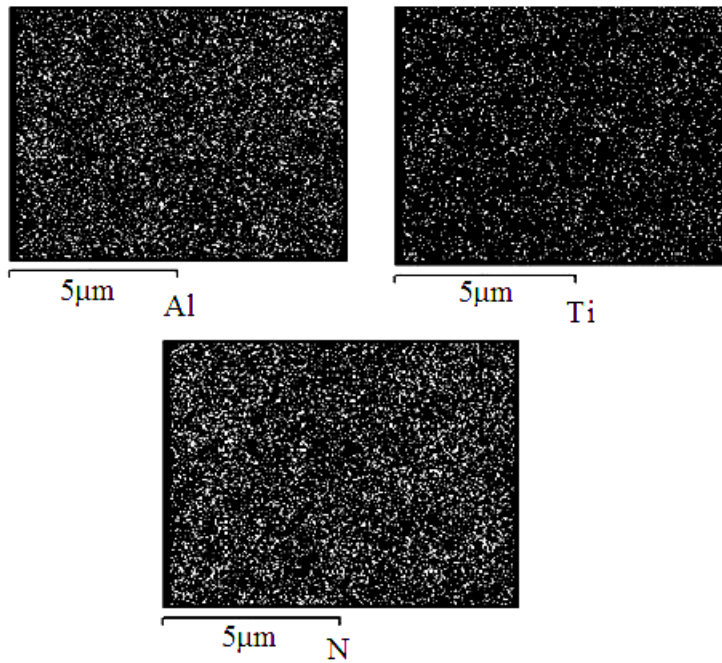


Figure 9: Layer Elements Dispersion

Contact Angle Test

One of the factors determining the wettability of a surface is the contact angle between the liquid and that surface. The contact angle of a liquid (droplet) is formed at the interface between a solid and that liquid at the point where the droplet contacts the solid surface. As the contact angle approaches zero, the wettability increases and as the contact angle increases, the wettability of the surface decreases.

If the tendency of water droplets to stick to themselves is more than their tendency to stick to a certain surface, that surface is called hydrophobic, and in this case, water contact angle is larger than 90 degrees. Conversely, if water droplets tend to stick to a surface, that surface is hydrophilic, and water contact angle is smaller than 90 degrees (Fig 10).

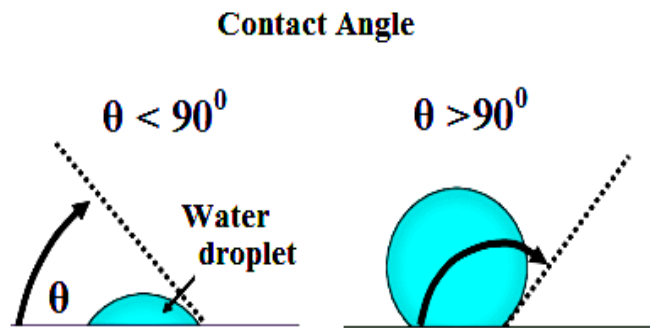


Figure 10: Contact angle between a droplet and a surface

The results of Contact Angle analysis showed that the contact angle between a water droplet and the steel substrate surface is 44.54° and the surface is hydrophilic. The TiAlN nanoparticles deposition results in an increase in the contact angle up to 100.62° , so, the steel surface is hydrophobic (Fig 11).

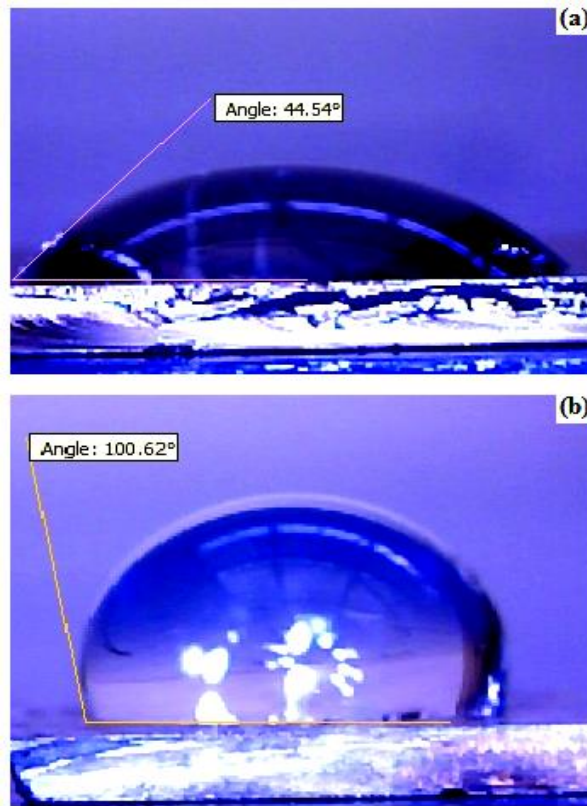


Figure 11: The contact angle between a droplet and the surface a) before TiAlN nanoparticles deposition and b) after TiAlN nanoparticles deposition

Micro-hardness Results

Micro-hardness is a mechanical property of thin layers, which relates to tensile strength. In this method, a square pyramid penetrator with 136° of apex angle is used. The penetrator penetrates in the sample surface with a given force and makes a rectangular sign with the diameters of d_1 and d_2 (Fig 12). Vickers hardness number (DPH) is calculated as Force/Penetrated Area. The penetrated area is calculated from microscopic lengths and diameters. Thus, we have

$$DPH = \frac{2P \sin\left(\frac{\theta}{2}\right)}{L^2} = \frac{1.854P}{L^2} \tag{2}$$

Where P is the force in kg, L is the mean length of the diameters in mm, and θ is the pyramid apex angle (i.e. 136°). Given the micro-hardness results, the hardness of the samples deposited at 100, 150, and 200 shots was 243, 260, and 286 VH, respectively.

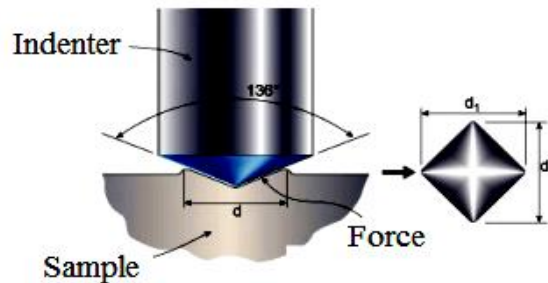


Figure 12: Schematic of Vickers Hardness

Conclusion

1. TiAlN Nano-particles were grown on Stainless Steel 316 sub-layer using 1.5kJ Mather Plasma Focus device.
2. XRD results indicated the formation of TiAlN structure on the sample surfaces, which is matched with the standard data for TiAlN.
3. According to SEM images and EDX analysis, an increase in the number of the shots resulted in a higher deposition on the sub-layer, increasing the size of the Nano-particles.
4. According to AFM images, the mean surface thickness is increased as the shots increase in number.
5. Contact Angle analysis shows the contact angle between the water droplet and the steel substrate surface 44.54° (hydrophilic) and the contact angle between the droplet and the surface of deposited TiAlN nanoparticles 100.62° (hydrophobic).
6. According to the micro-hardness results, the increased number of the shots increased the hardness of the deposited samples from 243 to 286 VH.

Reference

1. Ahlgren M., Blomqvist H., (2005).” Surface and Coating Technology”, 200, 157-160.
2. Aleksandar Miletić, Peter Panjan, Miha Čekada, Pal Terek, Lazar Kovačević, Branko Škorić, (2018).“TiAlN tribological coatings prepared in industrial deposition system with different rotations”, Advanced Technologies and Materials, Vol. 43, No. 2.
3. Hosseinnejad M.T., Ghorannevis Z., Soltanveisi M., Shirazi M., (2011). “Journal of fusion energy”, 516, 30.
4. Kim G., Lee S., Hahn J., (2005). “Surface and Coating Technology”. 193, 213-218.
5. Lee S.Y., Wang S.C., Chen J.S., Huang J.L., (2007). “Surface and Coating Technology”, 202, 977-9819.
6. Liu G.T., Duh J.G., Chung K.H., Wang J.H., (2005). “Mechanical characteristics and corrosion behavior of (Ti,Al)N coatings on dental alloys”, Surface and Coatings Technology, Vol. 200, No. 7, Pp. 2100–2105.
7. Rawat R.S., Lee P., White T., Ying L., (2001). “Surface and Coating Technology”, 4.134.
8. Shum P.W., Li K.Y., Zhou Z.F., Shen Y.G., (2004). “Surface and Coating Technology”, 185,245-253 J.
9. Tousif H., Riaz A., Jamil S. and Nida KH., (2011). “TiAlN coatings synthesized using a dense plasma focus system and varied focus shots”, Radiation Effects & Defects in Solids, Vol. 166, No. 11, Pp. 873-883.
10. Vikas Chawla, Amita Chawla, Y. Mehta, D. Puri, S. Prakash and Buta Singh Sidhu, (2011). “Journal of the Australian Ceramic Society” Volume 47[1], 48-55.
11. Wagner J., Edlmayr V., Penoy M., Michotte C., Mitterer C., Kathrein M., (2008). “Int. J. Refract. Metals Hard Mater”. 26,563.